CIRP Annals - Manufacturing Technology xxx (2018) xxx–xxx

Contents lists available at ScienceDirect

CIRP Annals - Manufacturing Technology

journal homepage: http://ees.elsevier.com/cirp/default.asp

Modelling of the combined microstructural and cutting edge effects in ultraprecision machining

M.A. Rahman [a], K.S. Woon [a,*], V.C. Venkatesh (1)[b], M. Rahman (1)[a]

[a] Department of Mechanical Engineering, National University of Singapore, 10, Kent Ridge Crescent, 119260, Singapore
[b] Department of Mechanical Engineering, University of Nevada, Las Vegas, 4505 S. Maryland Pkwy., Las Vegas, NV 89154, United States

ARTICLE INFO

Keywords:
Micro structure
Cutting edge
Finishing

ABSTRACT

The mechanics of ultraprecision machining (UPM) is known to be affected by materials microstructures and cutting tool geometries when cutting magnitudes are reduced to micron-scale. To model the combined effects, a flow stress model that correlates the grain size and chip thickness to the relative tool sharpness is first proposed. Subsequently a novel behavioural chip formation model is developed to distinguish the transitions in chip formation regimes due to the microstructural and cutting edge effects. This led to the discovery of a unique finishing regime where surface roughness is improved by 61.7%, 63.9% and 86.4% for Al-alloy, Mg-alloy and Cu-alloy respectively.

1. Introduction

The cutting magnitudes in UPM are usually in the micrometre or even nanometre range. At such fine cutting scales, tool-work interaction at the cutting edge is significantly more complex than conventional machining due to the finite edge sharpness [1] as shown in Fig. 1(a). Reducing cutting magnitudes down to the size of the cutting edge as shown in Fig. 1(b) and the size of the material grain as shown in Fig 1(c) gives rise to the cutting edge effects [2] and the microstructural effects [3] simultaneously. Without having good understanding of both effects as a whole, desirable surface finishing at the ultra-precision level is hard to obtain repeatedly.

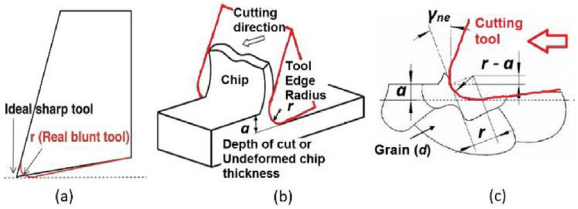

Fig. 1. Emergence of cutting edge effects: (a) ideal vs real tool [1] (b) depth of cut vs edge radius [2] (c) depth of cut vs material grain size [3].

This explains the needs for novel methods to improve surface quality for some UPM applications. For example, a synergistic cutting-burnishing strategy is applied to customize surface integrity of a biodegradable Mg–Ca alloy [4]. While a mechanical surface modification method involving the use of a reverse cutting tool with microgeometry on the edge was reported [5]. More recently, the feasibility in achieving similar 'burnished-like finishing' in the cutting of Al alloy was explored [6]. These studies show the great potential in improving surface finishing through a controlled surface burnishing mechanism, which is governed by the combined cutting edge and microstructural effects during tool-work interaction. To quantify cutting edge effects, the relative tool sharpness defined as the ratio of undeformed chip thickness a to cutting edge radius r. In our previous study on carbon steel using cemented carbide tools with $r = 10$ μm, the critical a/r range 0.20–0.25 was identified for the 'extrusion-like' mechanism to achieve the best surface finish [7]. To explore the cutting edge effects on other materials, a series of orthogonal cutting experiments were conducted on Al-alloy, Mg-alloy and Cu-alloy using CBN tools with $r = 12.6$ μm on Toshiba ULG-100C lathe by varying the feed rate to enforce variation in undeformed chip thickness as described [8]. Moreover, the grain size(d) was estimated from the material microstructures as shown in Fig. 2(a). For a nominal rake angle γ, the effective rake angle γ_{ne} is correlated with a/r according to Eq. (1) and the distribution trend is shown in Fig. 2(b).

$$\gamma_{ne} = \sin^{-1}(a/r - 1), \text{for } a \le r(1 + \sin\gamma) \quad (1)$$

The influence of microstructural effects on surface finishing, measured with Taylor Hobson Talysurf-120, is evident from the 'extrusion range' of different materials as in Fig. 2(b). The optimal or threshold range of a/r for minimum R_a is found to be decreasing with decreasing grain size (d). Furthermore, correlating material hardness and threshold range of a/r renders a graphical trend (red solid line) similarly obtained [9] as shown in Fig. 3 with a regression model $(a/r)_{\text{Threshold}} = 44.746(HV)^{-1.037}$, where the coefficient of determination $R^2 > 98\%$. The results thus indicate the significance of material property (i.e., hardness) and microstructural effects in UPM.

* Corresponding author.
E-mail address: mpewks@nus.edu.sg (K.S. Woon).

https://doi.org/10.1016/j.cirp.2018.03.019
0007-8506/

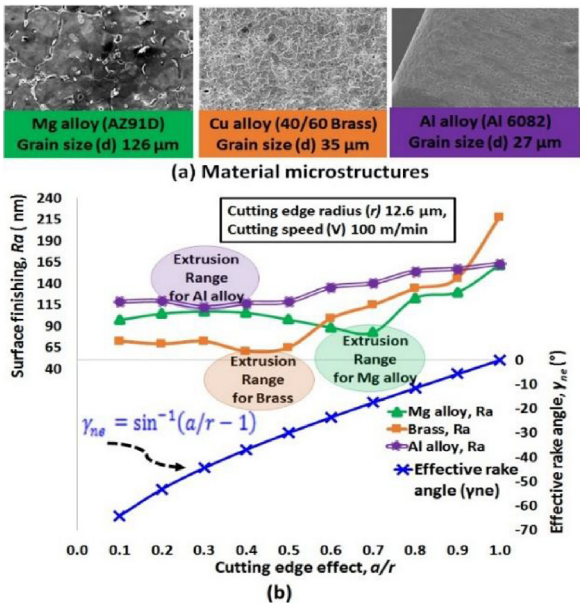

Fig. 2. Influence of workpiece microstructure on extrusion-like finishing range of Al, Mg and Cu-alloy for the cutting edge effects (a/r).

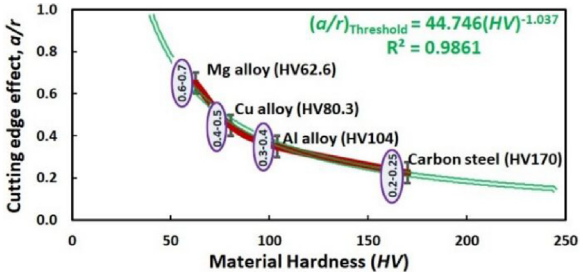

Fig. 3. Influence of material hardness on cutting edge effect (a/r).

Despite the significance of both microstructural and cutting edge effects, little is known about the mechanics of tool-work interaction to realize the surface burnishing mechanism. Due to this, a generic cutting model to ensure the productivity and repeatability of UPM in producing high quality surface finishing on a wider range of metallic materials is still lacking. This forms the objective of this study to establish quantitative understanding of both effects when combined on material flow stress, specific cutting energy, chip morphology and surface quality for Al-alloy, Mg-alloy and Cu-alloy. An analytical framework that accounts for the combined effects is thus proposed and substantiated with a series of cutting experiments to yield reasonable predictions.

2. Modelling approach

The behaviour of material 'pilled-up' akin to spherical indentation can be correlated to the material removal mechanism in UPM as illustrated in Fig. 4, in which metal cutting is performed at relatively fine scales.

The relationship between cutting edge geometry and material indentation behaviour is illustrated in Fig. 5. The solid red line ACD represents the permanent indentation after unloading, which resembles the cutting edge profile with edge radius OP. The green dotted line

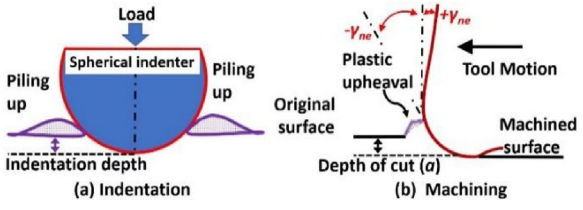

Fig. 4. Analogy of material piling up [10] and removal in UPM.

PQD describes the indentation profile of the cutting tool. The depth of penetration below the circle of contact h_p [10] can be calculated as:

$$h_p = r - \sqrt{(r^2 - x^2)} \tag{2}$$

where the contact radius (x) is obtained from the undeformed chip thickness a and cutting edge radius r as:

$$x = \sqrt{(2ra - a^2)} \tag{3}$$

The ratio of contact depth h_c and penetration depth h_p defined as c^2 in Ref. [11] is used to quantify the degree of piling-up. Moreover, the degree of indentation is correlated with yield stress σ_y and reduced modulus E_r by a single non-dimensional group $\Lambda = E^* x/r\sigma_y$ where the reduced modulus is related to the elastic modulus E_w, E_t and Poisson's ratio ν_w, ν_t of the workpiece and cutting tool as:

$$\frac{1}{E_r} = \frac{1-\nu_w^2}{E_w} + \frac{1-\nu_t^2}{E_t} \tag{4}$$

Using the material property of E/σ_y and Λ, the value of c^2 can be determined from the similarity solution graph as reported in Ref. [11] to determine the pile-up height Δp:

$$h_{pile\ up}(\Delta p) = h_c - h_p \tag{5}$$

Unloading a spherical indentation from the onset of full plastic flow leaves an impression in the surface with larger radius O′P′ (R) than indenter radius OP (r) with the following relationship [10]:

$$\frac{\Delta p}{2} = \left(\frac{x^2}{2}\right)\left(\frac{1}{r} - \frac{1}{R}\right) \tag{6}$$

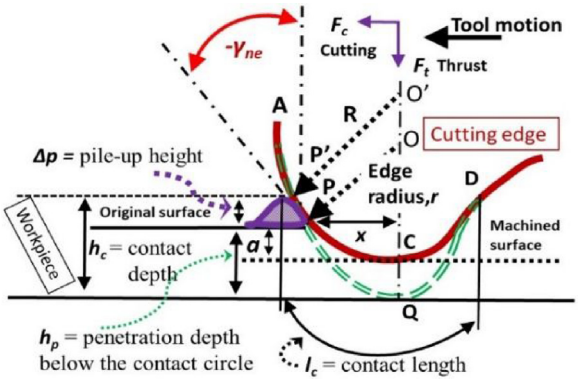

Fig. 5. Schematic of fine scale material removal mechanism in UPM.

For an applied tangential force in the horizontal direction [12] that is just sufficient to initiate sliding and pile-up above the initial metal surface, the coefficient of friction μ is correlated as:

$$\mu = \left(\frac{2}{\pi x^2}\right)\left(\frac{p'_m}{p_m}\right)\left[r^2 \sin^{-1}\frac{x}{r} - r\sqrt{(r^2 - x^2)}\right] + \left(\frac{4r}{\pi x^2}\right)\left(\frac{s}{p_m}\right)\left[r - \sqrt{(r^2 - x^2)}\right] \tag{7}$$

where p'_m, p_m and s are the dynamic flow pressure, maximum "static" flow pressure and shear stress per unit contact area respectively.

According to the surface layer model described in Fig. 6(a), surface grains are easier to rotate and slide, which leads to a reduction in flow stress. As the material grain size becomes comparable to cutting edge radius, a fraction of the grain d is thus removed while the intra-crystalline deformation arising from the generation of dislocations in the process across the crystal is illustrated in Fig. 6(b).

Therefore, crystal plasticity [15] is used to develop a flow stress model σ with material grain size d and chip thickness t_c:

$$\sigma = \left(M\tau_R + \frac{k_{HP}}{\sqrt{d}}\right) - (d/t_c)\left(M\tau_R + \frac{k_{HP}}{\sqrt{d}} - m\,\tau_R\right) + M\alpha_d G\sqrt{\frac{b\,k_b\,\theta_{av}}{d}} \tag{8}$$

Please cite this article in press as: Rahman MA, et al. Modelling of the combined microstructural and cutting edge effects in ultraprecision machining. CIRP Annals - Manufacturing Technology (2018), https://doi.org/10.1016/j.cirp.2018.03.019